

Integrated multiple patch-clamp array chip via lateral cell trapping junctions

J. Seo

Berkeley Sensor and Actuator Center, Department of Bioengineering, University of California, Berkeley, Berkeley, California 94720

C. Ionescu-Zanetti

Neuroscience Research Institute, University of California, Santa Barbara, Santa Barbara, California 93106

J. Diamond

Berkeley Sensor and Actuator Center, Department of Bioengineering, University of California, Berkeley, Berkeley, California 94720

R. Lal

Neuroscience Research Institute, University of California, Santa Barbara, Santa Barbara, California 93106

L. P. Lee^{a)}

Berkeley Sensor and Actuator Center, Department of Bioengineering, University of California, Berkeley, Berkeley, California 94720

(Received 10 October 2003; accepted 31 December 2003)

We present an integrated multiple patch-clamp array chip by utilizing lateral cell trapping junctions. The intersectional design of a microfluidic network provides multiple cell addressing and manipulation sites for efficient electrophysiological measurements at a number of patch sites. The patch pores consist of openings in the sidewall of a main fluidic channel, and a membrane patch is drawn into a smaller horizontal channel. This device geometry not only minimizes capacitive coupling between the cell reservoir and the patch channel, but also allows simultaneous optical and electrical measurements of ion channel proteins. Evidence of the hydrodynamic placement of mammalian cells at the patch sites as well as measurements of patch sealing resistance is presented. Device fabrication is based on micromolding of polydimethylsiloxane, thus allowing inexpensive mass production of disposable high-throughput biochips. © 2004 American Institute of Physics. [DOI: 10.1063/1.1650035]

Patch-clamp recording has had a profound impact on electrophysiology, by playing a crucial role in the characterization of cellular ion channels. Traditionally, patch-clamp recording is accomplished with a micromanipulator-positioned glass pipette under a microscope.¹ As illustrated in Fig. 1(a), a cell membrane patch is sucked into the glass pipette and forms a high electrical resistance seal. Current that passes through the ion channels in either the membrane patch or the whole cell membrane is then recorded at different bias voltages. The properties of ion channels are central to nervous systems and often act as targets for drugs.²

Despite constant improvements in the traditional patch-clamp technique, it remains laborious and requires precisely pulled pipettes to be placed in the vicinity of the cell by a skillful operator using a micromanipulator under a microscope. Because of these requirements, the patch-clamp technique has not been widely used in proteomics and drug discovery development, which demand high-throughput automated measurements. An automated patch-clamp setup for high-throughput measurements using disposable devices would eliminate the prohibitive investment of time of the traditional patch-clamp, while maintaining its advantages over other measurements.² Consequently, chip-based patch-clamp devices have been proposed using silicon oxide coated nitride membranes,³ silicon elastomers,⁴ polyimide films,⁵

quartz⁶ or glass⁷ substrates. Recently, three-dimensional structures more similar to patch pipettes have also been fabricated.⁸ All chip-based devices developed to date use the planar geometry shown in Fig. 1(b), where the patch pore is etched in a horizontal membrane that divides the top cell compartment from the recording electrode compartment.

Here we present the design, fabrication, and characterization of an integrated multiple patch-clamp array chip by utilizing lateral cell trapping junctions, as shown in Fig 1(c). This geometry dramatically reduces the capacitive coupling between the cell reservoir and the patch channel, an important feature for low noise channel recording. Since the patch channels are in the horizontal plane, multiplexed parallel patch sites that are only tens of μm apart are possible. In the current design, the distance between patch sites is a few hundred μm [Fig. 1(d)]. Channel binding drugs can therefore be administered in small volumes, while the effects on channel activity can be recorded in parallel at a number of patch sites. The whole device is fabricated using micromolding of polydimethylsiloxane (PDMS), a high-throughput, inexpensive procedure.

The fabrication steps are presented in Figs. 2(a)–2(f). A silicon mold was prepared using surface micromachining techniques. First, 3.1 μm height patterns were made to define the narrow patch channels using deep reactive ion etching [Fig. 2(a)]. Second, 50 μm high patterns were added for wide connection regions using SU-8 negative photoresist

^{a)}Electronic mail: lplee@socrates.berkeley.edu

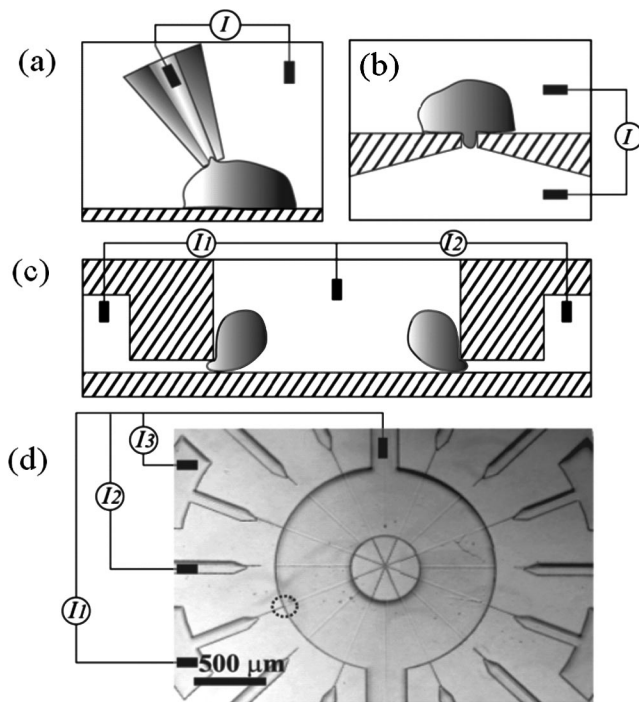


FIG. 1. Comparison of patch-clamp setups: (a) Traditional patch-clamp based on a glass micropipette. (b) On-chip planar patch clamp. (c) Microarray design with patch channels on the sides of a large central channel for cell delivery. A section containing two patch sides is shown. (d) Top view of the patch-clamp array device (optical microscope image) showing the center channel and 14 radial patch channels. The connectivity of the reference electrode and three of the patch electrodes is shown schematically. The small circle indicates one of the patch sites.

[Fig. 2(b)]. After a base and a curing agent of PDMS were mixed (1:10), the liquid mixture was then poured onto the mold and cured at 80 °C for 1 h. Scanning electron microscopy (SEM) images of the fabricated device are shown in Figs. 2(g) and 2(h). Despite the fact that fabrication should result in a square patch orifice, we observe that the top of the orifice is rounded. Rounding of the top of the orifice is a beneficial artifact of mold fabrication, and we observe the channel top is rounded next to the patch orifice in the mold [Fig. 2(i)]. When SU8 is selectively polymerized in order to create the large channels on top of the small patch channel defined in Si, light scattering near the Si surface results in deviation from the intended vertical SU8 wall. The resulting rounded feature at the bottom of the SU8 wall [Fig. 2(i), arrow A] is also present on top of the small Si wall [Fig. 2(i), arrow B], resulting in rounding of the top of the patch orifice. This feature is reproducible since it is observed to be part of the mold geometry at every patch orifice. For fluidic connections to outside tubing, 0.5 mm holes were punched mechanically into the cured detached PDMS device. The device was subsequently bonded to a thin PDMS layer which was spin cast and then cured onto a glass substrate. Finally, plastic tubes were connected to the reservoirs, via punched holes, to load both cells and electrolyte solutions and to apply suction to the patch channel.

A human tumor cell line (HeLa), 12–17 μm in diameter, was used for seal resistance experiments. Before introducing the cells, the fluidic network was filled with phosphate buffered saline (PBS), taking care to expel all air bubbles. The electrical connection between the reference Ag/AgCl elec-

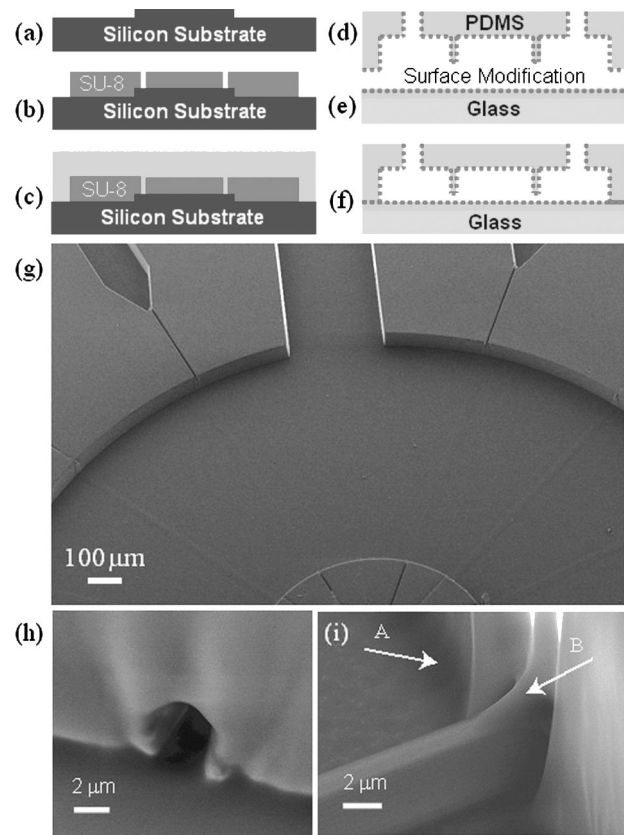


FIG. 2. Fabrication of the patch-clamp microarray. The Si etch (a) is used to define the patch channels (4 μm×3.1 μm), while SU-8 photoresist (b) is used to define the large access channels (50 μm high). After PDMS is cured (c) the devices are detached and mechanically punched. The (d) devices and the (e) glass substrate precoated with a thin PDMS layer are treated with oxygen plasma. (f) The devices are bonded to the thin PDMS. SEM images of the overall device geometry before bonding (upside down) and a closeup of the patch pore after bonding are shown in (g) and (h), respectively. (i) SEM image of the mold.

trode in the main channels and the patch electrode in the lateral patch channel was confirmed by applying a 20 mV square pulse and recording the current response. A typical channel current response is shown in Fig. 4(a), indicating a channel resistance of 10–14 MΩ. This is comparable to the access resistance of traditional micropipettes, but can be reduced by altering the channel geometry. After dissociation by trypsin treatment, cells were suspended in PBS and injected into the main channel. Gentle pressure (1 psi) was applied to the patch channel while cells were loaded into the main fluidic channel in order to prevent contamination at the patch site. A cell can either be trapped randomly or selectively by controlling the flow through the main fluidic channel. A cell found within 100–200 μm of the patch channel opening can be trapped within a 1 s time interval by applying 2 psi of negative pressure to the patch channel (Fig. 3). Right after trapping the cell, negative pressure was removed and the cell was allowed to form a seal with the rim of the patch channel. The top down view allows effective visualization of the membrane protrusion into the patch channel.

Patch resistance was recorded by applying a square voltage pulse of amplitude 20 mV and 50 ms duration. The current response was recorded using a standard patch-clamp amplifier (Dagan PC-ONE, Minneapolis, Minnesota) and low

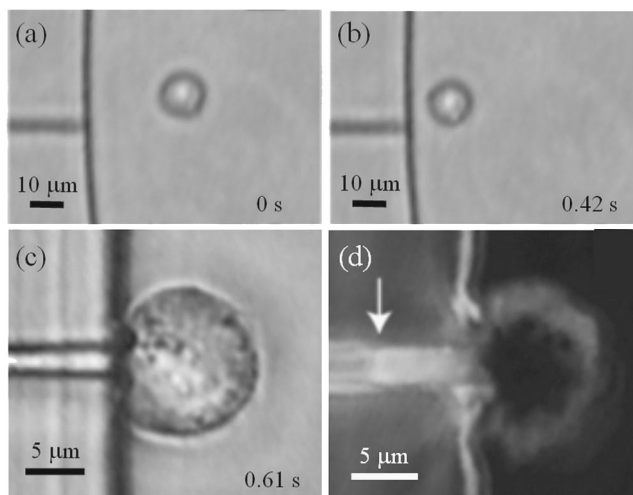


FIG. 3. (a)–(c) Three sequential images showing a HeLa cell being trapped by applying negative pressure (2 psi) to the patch channel. The third frame is magnified in order to show cell positioning on the patch pore. (d) Real time observation of cell membrane deformation.

pass filtered at 1 kHz. The current response presented contains no capacitance compensation. The resistance of the open patch channel was measured to be 14 ± 4 M Ω . The channel geometry ($4 \mu\text{m} \times 3.1 \mu\text{m} \times 200 \mu\text{m}$) and the conductivity of the electrolyte used ($\sigma = 1$ S/m) yield a calculated resistance of 17 M Ω , in reasonable agreement with the measurement. Capacitive coupling leads to a spike in current when the bias voltage is first applied (Fig. 4). Integrating spike currents gives an approximation of the charge stored in the capacitor, $q = \int Idt$. Capacitance can then be calculated by using $C = q/V$. This capacitance measurement method yielded a capacitance of 10 ± 1 pF for connections between the device and the patch-clamp amplifier input, but showed no further increase in capacitance when the device itself was attached. We can conclude that the device capacitance is within measurement error, or $C_{\text{dev}} \leq 1$ pF. Our calculations, using the device geometry and $\epsilon_{\text{PDMS}} = 2.46$,⁹ yielded a predicted device capacitance of $C_{\text{dev}} = 0.5$ fF. By comparison, capacitances for micromachined patch-clamp devices are 30 pF for micronozzle devices⁸ and 1 pF for glass substrates,⁶ while micropipette capacitances are in the range of $2 \text{ pF} \leq C_{\text{pipette}} \leq 20 \text{ pF}$.

Cell trapping by suction was described earlier in this letter. The current response from the cell by a 20 mV/50 ms current pulse is shown in Fig. 4(b). The calculated sealing resistance after attaching the cell was 140 M Ω . Typical seal resistances were in the range of 140 ± 20 M Ω , while 200 M Ω was the highest seal resistance obtained. By applying positive pressure to the patch-clamp channel, the trapped cell was expelled from the channel. As soon as the cell was expelled, the current response returned to that of the open channel. Subsequent cell trapping in the same channel resulted in lower seal resistance, presumably due to contamination at the opening of the patch channel.

In summary, an integrated multiple patch-clamp array

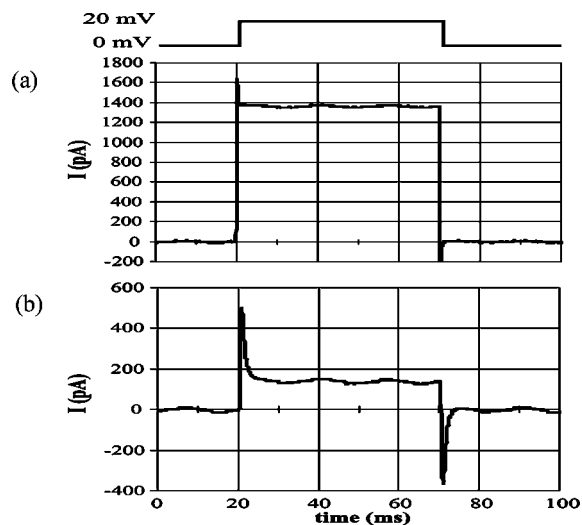


FIG. 4. Device current response to a 20 mV voltage pulse (a) before and (b) after cell trapping. In (a), the channel impedance is 14 M Ω , while in (b) the average seal resistance is 144 ± 3 M Ω .

chip via reliable lateral cell trapping junctions is presented. The intersectional design of the microfluidic network provides instantaneous multiple cell addressing. The geometry of this device not only minimizes capacitive coupling between the cell reservoir and the patch channel, but also allows simultaneous optical and electrical characterizations for studying roles of ion channels with respect to cellular functions. The device geometry, together with the low dielectric constant of PDMS, results in very low capacitive coupling between the cell reservoir and the patch channel: $C_{\text{predicted}} = 0.4$ fF and $C_{\text{measured}} \leq 1$ pF. The lateral design also allows efficient multiplexing of patch measurements, exchange of intracellular electrolytes while the cell is attached to the patch pore, and optical observation of membrane deformation. While measured seal resistances are not yet high enough for single channel measurements ($R = 140 \pm 20$ M Ω), they should be sufficient for loose patch measurements. Future improvements in PDMS surface treatment and patch pore geometry should lead to increases in seal resistance. This device has the potential for high-throughput, low cost cell-based patch-clamp measurements.

¹B. Sakmann and E. Neher, *Single Channel Recording* (Plenum, New York, 1983).

²J. Xu, X. B. Wang, B. Ensgn, M. Li, A. Guia, and J. Q. Xu, *Drug Discovery Today* **6**, 1278 (2001).

³N. Fertig, A. Tilke, R. H. Blick, J. P. Kotthaus, J. C. Behrends, and G. ten Bruggencate, *Appl. Phys. Lett.* **77**, 1218 (2000).

⁴K. G. Klemic, J. F. Klemic, M. A. Reed, and F. J. Sigworth, *Biosens. Bioelectron.* **17**, 597 (2002).

⁵A. Stett, V. Bucher, C. Burkhardt, U. Weber, and W. Nisch, *Med. Biol. Eng. Comput.* **41**, 233 (2003).

⁶N. Fertig, R. H. Blick, and J. C. Behrends, *Biophys. J.* **82**, 3056 (2002).

⁷N. Fertig, M. Klau, M. George, R. H. Blick, and J. C. Behrends, *Appl. Phys. Lett.* **81**, 4865 (2002).

⁸T. Lehnert, M. A. M. Gijs, R. Netzer, and U. Bischoff, *Appl. Phys. Lett.* **81**, 5063 (2002).

⁹Z. Lin, T. Kerle, and T. P. Russel, *Macromolecules* **35**, 3971 (2002).